

# Direct Power Control Applied on 5-Level Diode Clamped Inverter Powered by a Renewable Energy Source

A. Elnady

**Abstract**—This paper presents an improved Direct Power Control (DPC) scheme applied to the multilevel inverter that forms a Distributed Generation Unit (DGU). This paper demonstrates the performance of active and reactive power injected by the DGU to the smart grid. The DPC is traditionally operated by the hysteresis controller with the Space Vector Modulation (SVM) which is applied on the 2-level inverters or 3-level inverters. In this paper, the DPC is operated by the PI controller with the Phase-Disposition Pulse Width Modulation (PD-PWM) applied to the 5-level diode clamped inverter. The new combination of the DPC, PI controller, PD-PWM and multilevel inverter proves that its performance is much better than the conventional hysteresis-SVM based DPC. Simulations results have been presented to validate the performance of the suggested control scheme in the grid-connected mode.

**Keywords**—Direct power control, PI controller, PD-PWM, and power control.

## I. INTRODUCTION

THE distributed generation systems (DGS) have been penetrating distribution systems to form the core of the smart grid, where the power flow may be bi-directional. This penetration is greatly required because of the continuous increase of load demands and lacking the adequate generation capacity from the upstream systems. The DGU's capacity ranges from few tens KVA to few MVA [1]. Also, recent technologies for the DGU have been introduced to replace the traditional DGU. These technologies depend on the inverter circuit supplied by a renewable energy source such as solar PV and wind [1]. The main aim of the DGS is to inject the active and reactive power to meet the extra requirements of the existing loads. The aforementioned issues stipulate efficient and robust control schemes for the utilized inverter based DGS.

The DPC is developed from the traditional direct torque control, which is dedicated for the machines operation [2]. Afterwards, the DPC is used for DC rectifiers [3], [4]. Eventually, the DPC has been evolved to be applied on the DGS [5]-[9] in a grid-connected mode. The DPC mainly depends on the estimation of the feedback power [5]-[7] in the  $\alpha$ - $\beta$  stationary frame or the d-q rotating frame. This estimated power is compared to the power references. Then, the power error goes to the hysteresis controller in the  $\alpha$ - $\beta$  frame to drive

the SVM based 2-level or 3-level inverter circuit.

The Hysteresis-SVM based DPC suffers from several drawbacks such as chattering (oscillation) in the output power and variable switching frequency, and much injected harmonics coming from the 2-level inverters and 3-level inverter [5]-[9]. Several modified versions of the DPC have been proposed to improve the performance of the DPC's outputs, and alleviate its traditional drawbacks. A virtual flux based estimation process is introduced to estimate the feedback power [10], in which the accuracy of power estimation is improved. Another modification to the DPC has been introduced to use look-up-table for the SVM in order to stabilize its switching frequency [11]. Also, the sliding mode control is integrated with the DPC to improve its transient and steady state performance at different operating conditions [12]. The LCL filter is employed with the DPC in order to isolate high-frequency harmonics and third-order harmonic [13]. To improve the power estimation, a new version of power estimation based on a feedback linearization is introduced to improve the performance of the DPC [14]. Several versions of predictive control are merged with the DPC to improve and stabilize the performance of the SVM [15], [16].

This research is motivated by the drawbacks of the Hysteresis-SVM based DPC applied to the conventional inverter. Simply, the contribution of this work is exemplified for the following points:

- 1- The utilization of the 5-level diode clamped inverter makes the injected harmonics much less than the harmonics injected by the 2-level and 3-level inverter. The impact of this multilevel inverter will be shown in the power curve of the proposed technique.
- 2- The utilization of the PD-PWM with the diode clamped inverter is much easier and simpler than the utilization of the SVM with the same inverter [17]. It is noteworthy mentioning that the traditional DPC depends on the SVM for only 2-level and 3-level inverters.
- 3- The utilization of the PI controller improves the transient and steady state performance of the DPC. It is important to mention that the traditional DPC does not depend on the PI controller, but it relies on a combination of the hysteresis controller and the SVM.

This paper consists of five sections, the second section shows the mathematical formulation for the presented DPC; the third section gives detailed information about the utilized 5-level diode clamped inverter along with its switching

operation. The fourth section demonstrates the simulation results to prove the capability of suggested control scheme compared to the conventional DPC. The last section concludes the results and the findings of this paper.

## II. PROPOSED DIRECT POWER CONTROL

This section shows the conventional DPC associated with the proposed DPC. Both versions of the DPC are developed with help of the distribution system given in Fig. 1.

The renewable energy source of Fig. 1 (a) is already clarified in Fig. 1 (b) since it generates DC electric power from a clean source of energy and process this energy in a such way to make it ready for further utilization. The utilized energy source starts with receiving the solar energy and converts it to electric power through the Photovoltaic (PV) panels. The output electric power of the PV panels is also stored in batteries and a supercapacitor and consequently processed to be ready for utilization in power grids or in a standalone system with DC loads.

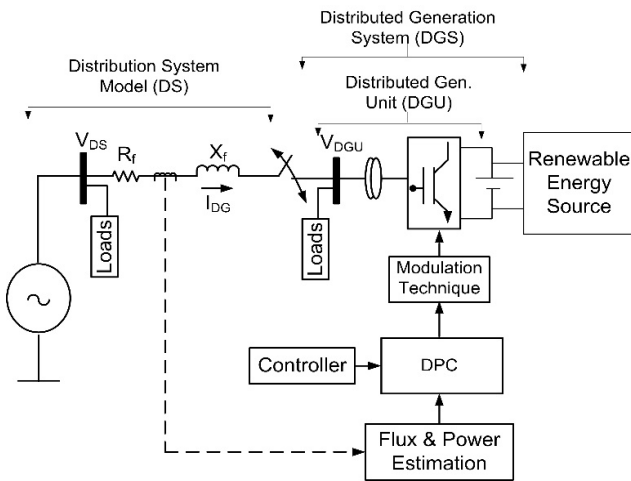


Fig. 1 (a) Distribution system under study

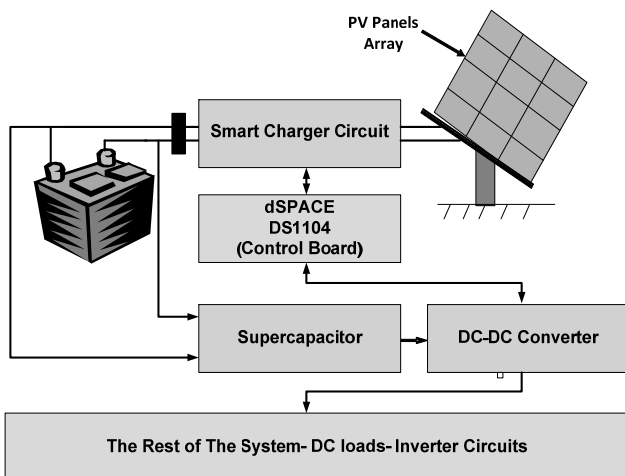


Fig. 1 (b) Renewable energy source

Fig. 1 Distribution system along with DGS

### A. The Conventional Direct Power Control

The system of Fig. 1 is used to derive the formulation of the DPC, in which the output power is controlled by two separate loops. In each control loop, the power reference is compared to the feedback power that is estimated by calculating the voltage in the  $\alpha$ - $\beta$  frame as,

$$\begin{bmatrix} V_{L\alpha} \\ V_{L\beta} \end{bmatrix} = \sqrt{\frac{2}{3}} \begin{bmatrix} 1 & \frac{1}{2} \\ 0 & \frac{\sqrt{3}}{2} \end{bmatrix} \begin{bmatrix} V_{ab} \\ V_{bc} \end{bmatrix} \quad (1)$$

A flux based estimation process is introduced, [10], to simplify the power estimation. This flux converter is obtained as,

$$\begin{bmatrix} \psi_{L\alpha} \\ \psi_{L\beta} \end{bmatrix} = \begin{bmatrix} \int V_{L\alpha} dt \\ \int V_{L\beta} dt \end{bmatrix} \quad (2)$$

$$\theta_\psi = \tan^{-1} \left( \frac{\psi_{L\beta}}{\psi_{L\alpha}} \right) \quad (3)$$

The flux is being converted from the  $\alpha$ - $\beta$  stationary frame into the d-q rotating frame as,

$$\begin{bmatrix} \psi_d \\ \psi_q \\ \psi_0 \end{bmatrix} = \begin{bmatrix} \cos(\omega t + \theta_\psi) & \sin(\omega t + \theta_\psi) & 0 \\ -\sin(\omega t + \theta_\psi) & \cos(\omega t + \theta_\psi) & 0 \\ 0 & 0 & 1 \end{bmatrix} \begin{bmatrix} \psi_{L\alpha} \\ \psi_{L\beta} \\ \psi_{L0} \end{bmatrix} \quad (4)$$

The apparent power received or injected by the Distribution System (DS) is defined as,

$$S = V_{DS} * I_{DS}^* \quad (5)$$

The voltage is defined in terms of the flux converter as,

$$V_{DS} = \frac{d|\psi_{DS}|}{dt} e^{j\omega t} + |\psi_{DS}| \omega e^{j\omega t} \quad (6)$$

In the d-q rotating frame if the  $|\psi_L|$  is synchronized with the d-axis, then  $|\psi_L|$  is constant and its derivative is zero. Then, first term of (6) goes to zero and the second term stays. The measurement that can be conducted in this research is the current  $I_{DG}$ , where the voltage at the distribution system is well known along with its flux  $\bar{\psi}_{DS}$ . The active and reactive power in the d-q rotating frame is defined as,

$$\begin{aligned} P &= k(V_{DS-d} I_{DG-d} + V_{DS-q} I_{DG-q}) \\ Q &= k(V_{DS-q} I_{DG-d} - V_{DS-d} I_{DG-q}) \end{aligned} \quad (7)$$

where  $k$  is a constant. Substituting (6) in (7) leads to the estimation of the active and reactive power received by DS as,

$$P_{estimated} = \frac{d\psi_{DS-d}}{dt} I_{DG-d} + \omega\psi_{DS-d} I_{DG-q}$$

$$Q_{estimated} = -\frac{d\psi_{DS-d}}{dt} I_{DG-q} + \omega\psi_{DS-d} I_{DG-d}$$
(8)

The output active power and reactive power are estimated from (8) and compared to the power reference. The power difference goes to the hysteresis controllers, which drive the SVM as shown in Fig. 2. The required number of switching sectors to operate the 5-level inverter is 96. These switching sectors along with the switching table for the 5-level inverter are already given in [17].

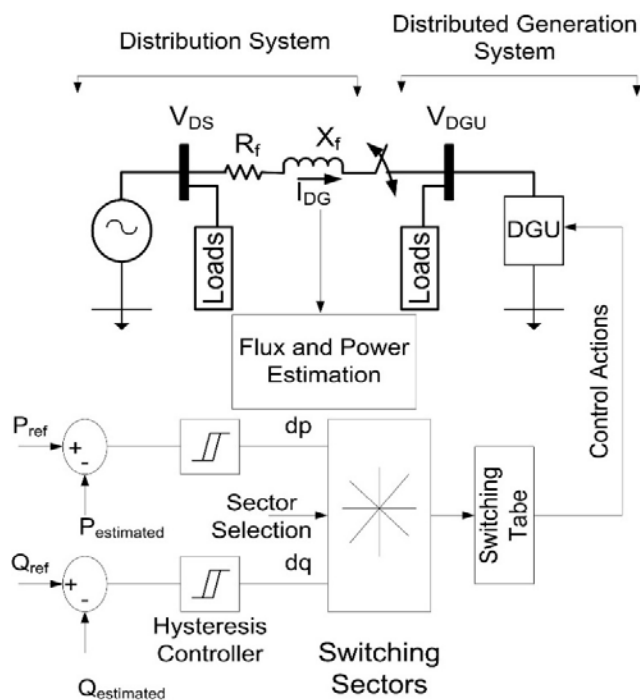


Fig. 2 Control block diagram of conventional DPC

### B. The Proposed Direct Power Control

The proposed DPC has almost the same structure of the conventional DPC shown in Fig. 2, but some changes have been interjected to the basic scheme to improve its performance. These changes are summarized as,

- 1- The hysteresis controller of Fig. 1 is replaced by a PI controller, which is much more efficient for controlling the transient and steady state performance.
- 2- The SVM is replaced by the PD-PWM, which is much more simpler and easier for the operation of the multilevel inverter.
- 3- The 2-level inverter or 3-level inverter of the DGU is replaced by the 5-level diode clamped inverter in order to

minimize the injected harmonics and distortion.

The proposed DPC is illustrated in Fig. 3, in which the output of the PI controller is used to develop the control signal for the PD-PWM since the outputs of the PI controllers in both loops are  $E_{DG-d-set}$  and  $E_{DG-q-set}$ , which are used to generate the control signal by converting  $E_{DG-d-set}$  and  $E_{DG-q-set}$  from the d-q frame to the a-b-c frame using inverse park transformation.

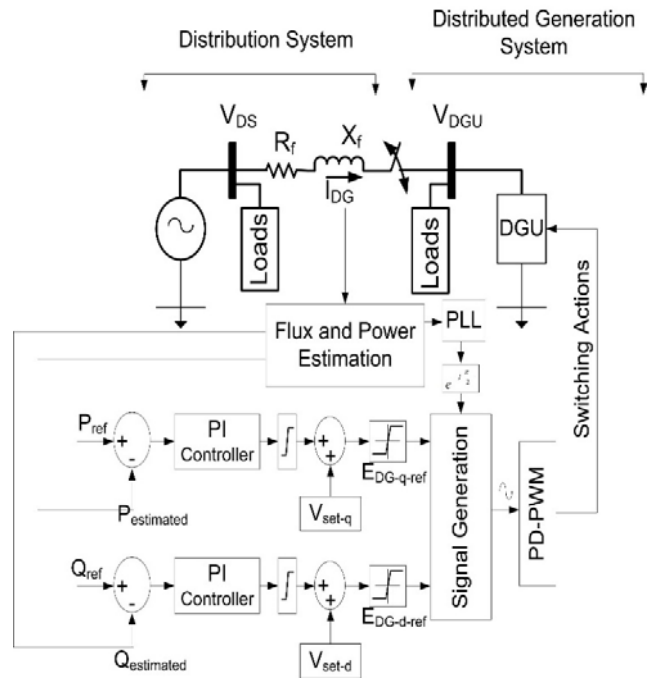


Fig. 3 The proposed DPC scheme

### III. INVERTER BASED DGU

The adopted inverter circuit is based on the 5-level diode clamped inverter. This structure is operated by Phase Disposition multi-carrier PWM, (PD-PWM) [17]. The PD-PWM for the 5-level diode clamped inverter encompasses four carrier triangular signals and one control signal. The carrier signals are shift in magnitude such that they extend from +1 V to -1 V, and the control signal is developed from the proposed PI as explained earlier. The details of operation and output performance for this 5-level diode clamped inverter are given in [18].

The multilevel inverter is intentionally utilized in this research to easily minimize the harmonic injection and efficiently suppress its harmonics. The structure and output of the inverter without filters of the 5-level inverter is given in Fig. 4. The inverter is supplied from four equal DC sources, that is why it gives five different levels in its output voltage. The output voltage before the transformer and the output voltage after the filter and transformer are given in Fig. 5. The THD after the filter is 1.4%.

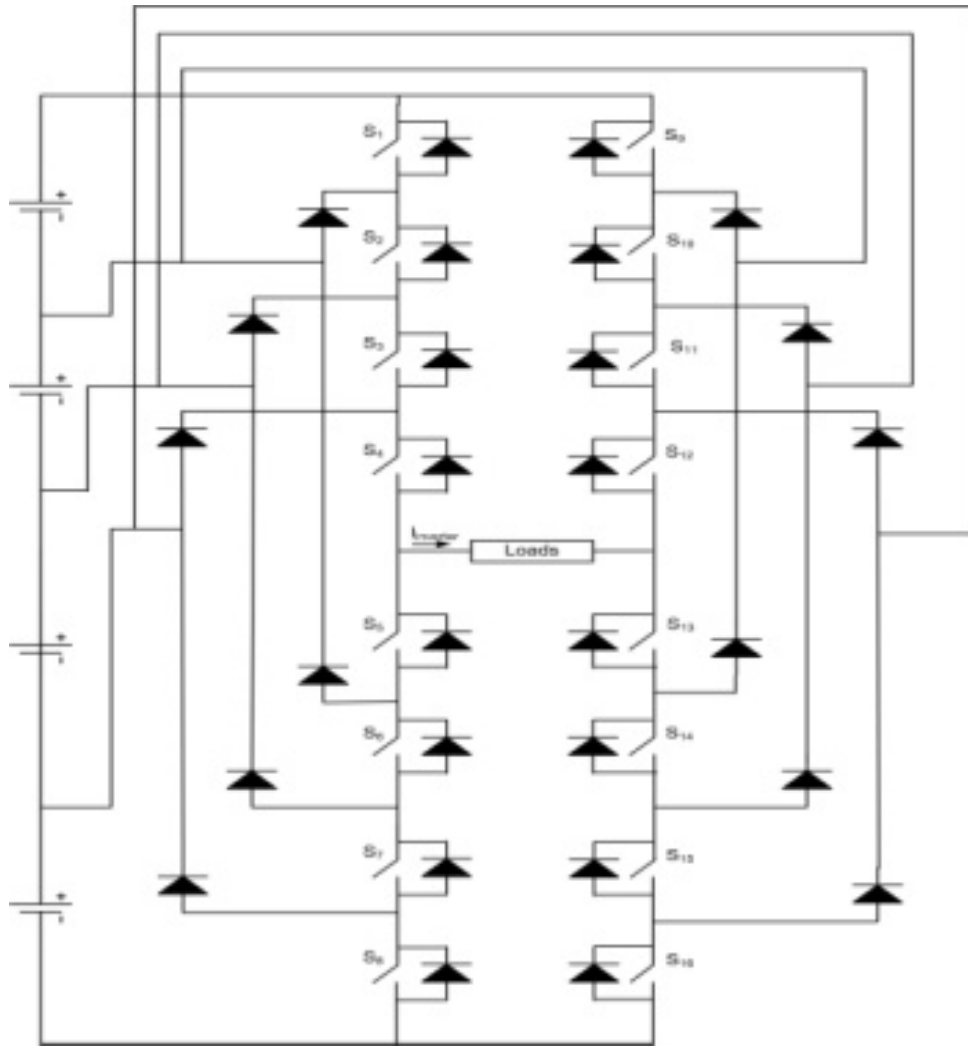


Fig. 4 The structure of 5-level diode clamped inverter

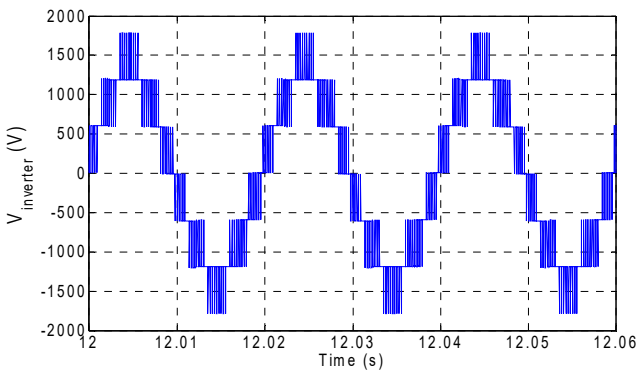


Fig. 5 (a) Voltage before the filter and transformer

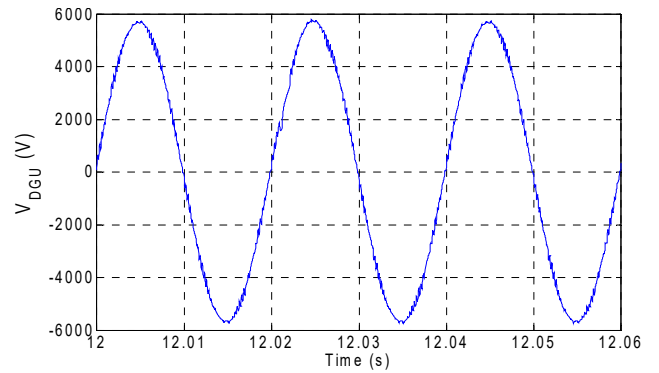


Fig. 5 (b) Voltage after the filter and transformer

Fig. 5 Voltages before and after the filter and transformer

#### IV. SIMULATION RESULTS

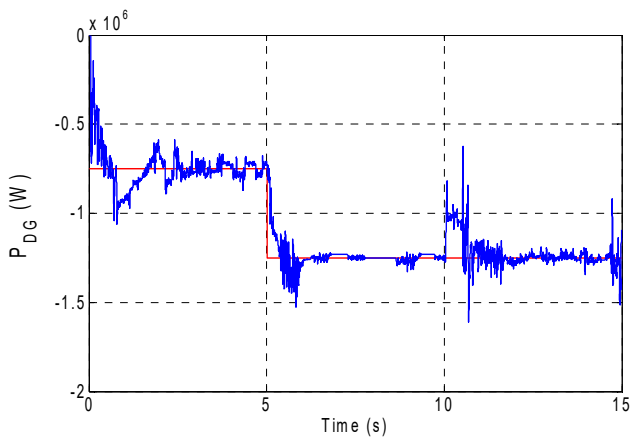
The presented results in this section include the simulation for the Hysteresis-SVM based DPC in comparison with the performance of the proposed PI-PD-PWM based DPC. The system under study for all simulation results is already given

in Fig. 1 whose parameters are listed as follows:

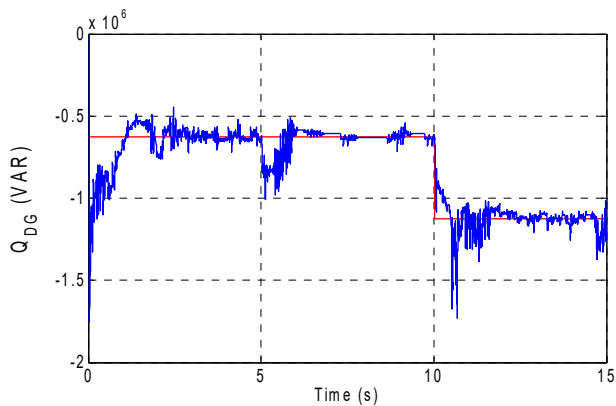
- The voltage level is 6.6 kV.
- Total loads take  $P = 0.244$  pu and  $Q = 0.154$  pu.
- The transformer is star-delta, with a ratio 1:5 and rating of 2.5 MVA.
- Transformer impedance is  $0.05+j0.1 \Omega$ .
- Distribution feeder impedance is  $0.0667+j0.345 \Omega/\text{km}$  for the length of 7.5 km
- For active power control loop and setting of PI controller are  $K_p=1250/2.5 \times 10^6$  and  $K_i=35000/2.5 \times 10^6$ .
- For reactive power control loop and setting of PI controller are  $K_p=1250/2.5 \times 10^6$  and  $K_i=35000/2.5 \times 10^6$

#### A. Results of the Hysteresis-SVM Based DPC

This section demonstrates the performance of the Hysteresis-SVM based DPC for its control scheme given in Fig. 2. The active power and reactive power are illustrated in Figs. 6 (a) and (b) respectively associated with power references. It is clear from power performance that the chattering and oscillation are the major problem for this Hysteresis-SVM based DPC. In addition to chattering, the decoupling between the active power loop and reactive power loop has a moderate performance since any change in one power influences the other power as shown in Fig. 6.



(a) Injected active power by SVM\_based DPC



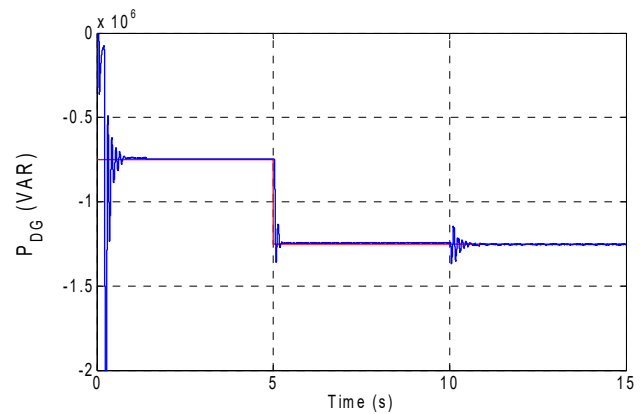
(b) Injected active power by SVM\_based DPC

Fig. 6 Active and reactive power performance by SVM based DPC

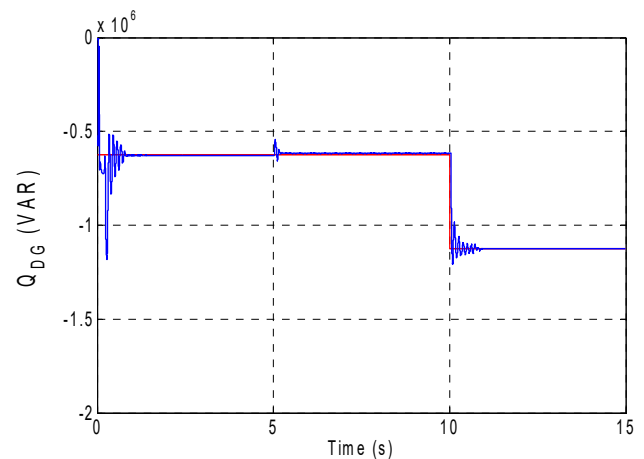
#### B. Results of the PI and PD-PWM Based DPC

This section shows the results of the proposed DPC, (a new combination of the PI controller, 5-level diode clamped inverter operated by PD-PWM), for the DGS in a grid-connected mode. The PI parameters are adjusted after several iterations in order to reach the optimum performance, which are  $K_p = 1.25 \times 10^3 / 2.5 \times 10^6$  and  $K_i = 35 \times 10^3 / 2.5 \times 10^6$  for both loops. The active power and reactive powers are displayed in Figs. 7 (a) and (b) respectively for the same power references of Fig. 6.

The performance of the proposed scheme is much better than that of the Hysteresis-SVM based DPC. This better performance is exemplified in the steady state performance, which indicates almost zero error power without chattering or a noticeable oscillation. The transient performance suffers from a little overshoot but it dies out very fast within 0.2 s.



(a) Magnitude of the control signal for the operation in Fig. 5

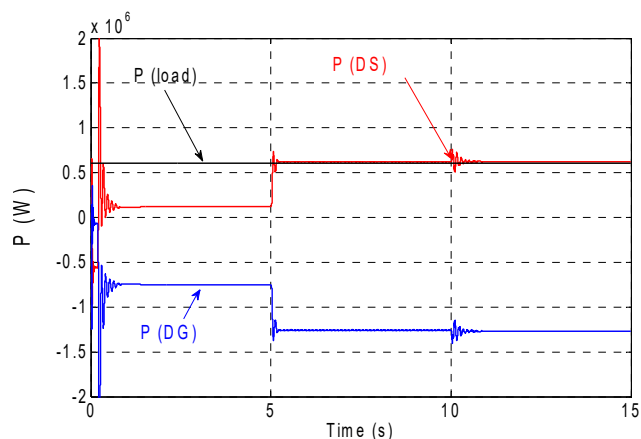


(b) Angle of the control signal for the operation in Fig. 5

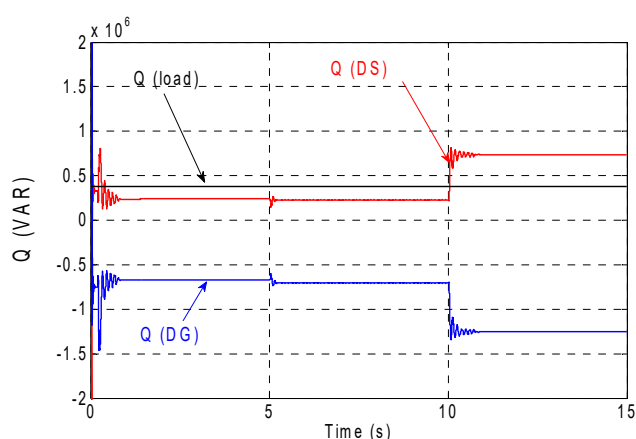
Fig. 7 Active and reactive power performance by proposed DPC

IEEE Std. 1547-2011 stipulates that the existence of the DGS helps the distribution system supply the loads with the required active and reactive power. The impact of the DGS on the distribution system/smart grid is exemplified in Fig. 8, where the active power and reactive power of the DGS, loads

and DS are shown in Figs. 8 (a) and (b) respectively for the same power performance of Fig. 7. It is clear that the injected power by the DGS, with negative sign, goes to the loads and the surplus goes back the distribution system, with positive sign. This clarifies the importance of the DGS in any distribution system, which forms the concept of the smart grid.



(a) Active power for distribution system, DG, and loads



(b) Reactive power for distribution system, DG, and loads

Fig. 8 Impact of DGS on distribution system

## V. CONCLUSION

This paper presents an improvement of the conventional DPC, (Hysteresis-SVM based DPC). This improvement is articulated for the utilization of a new combination of the PI controller and the 5-level inverter operated by the PD-PWM. The transient and steady state performance reveals that the overall performance of the proposed DPC is much better than the performance of the Hysteresis-SVM based DPC in terms of the chattering of the output power at steady state and overshoot of its transient performance. This presented control scheme controls the DGS to form the base for the smart grid, where a certain amount of power can transfer from one load side to another load side and the upstream distribution system.

## REFERENCES

[1] W. El-Khattam, and M. M. A. Salama, "Distributed Generation

Technologies, Definitions and Benefit," *Journal of Electric Power System Research*, vol. 71, pp. 119-128, 2004.

[2] M. P. Kazmierkowski, A. Kasprowicz, "Improved direct torque control flux vector control pf PWM inverter fed induction motor drives," *IEEE Transactions on Industrial Electronics*, vol. 42, pp. 344-350, 1995.

[3] M. Malinowski, M. Jasinski, M. P. Kazmierkowski, "Simple direct control of three-phase PWM rectifier using space-vector modulation (DPC-SVM)," *IEEE Trans. on Industrial Electronics*, vol. 51, no. 2, pp. 447-454, 2004.

[4] Z. Boudries, D. Ziani, M. Sellami, "Direct power control of a PWM rectifier fed autonomous induction generator for wind energy applications," *Journal of Energy Procedia, Elsevier*, vol. 36, pp. 391-400, 2013.

[5] L. Xu, D. Zhi, L. Yao, "Direct power control of grid connected voltage source converters," *Proc. Power Engineering Society General Meeting, USA*, pp. 1-6, 2007.

[6] T. Noguchi, K. S. Tomiki, I. Takahashi, "Direct power control of PWM converter without power-source voltage sensors," *IEEE Trans. on Industry Applications*, vol. 34, no. 3, pp. 473-479, 1998.

[7] R. Zaimeddine, T. Undeland, "Direct power control strategies of a grid-connected three-level voltage source converter VSI-NPC," *Proc. of 14th European Conference on Power Electronics and Applications, EPE* pp. 1-6, 2011.

[8] M. Monfared, M. Sanatkar, S. Golestan, "Direct active and reactive power control of single-phase grid-tie converters," *Proc. of IET on Power Electronics*, vol. 5, no. 8, pp. 1544-1550, 2012.

[9] J. Alonso-Martínez, J. Eloy-García, S. Arnaltes, "Direct power control of grid connected PV systems with three level NPC inverter," *Journal of Solar Energy, Elsevier*, vol. 84, pp. 1175-1186, 2010.

[10] A. Djerioui, K. Aliouane, M. Aissani, F. Bouchafaa, "Direct power control strategy for PWM rectifier with the function of an active based on a novel virtual flux observer," *Journal of Electric Engineering*, pp.1-8, 2012.

[11] D. Zhi, L. Xu, B. W. Williams, "Improved direct power control of grid-connected DC/AC converters," *IEEE Trans. on Power Electronics*, vol. 24, no. 5, pp. 1280-1292, 2009.

[12] L. Shang, "Sliding-mode-based direct power control of grid-connected wind-turbine-driven doubly fed induction generators under unbalanced grid voltage conditions," *IEEE Trans. on Energy Conversion*, vol. 27, no. 2, pp. 362-373, 2012.

[13] L. A. Serpa, J. W. Kolar, S. Ponnaluri, P. M. Barbosa., "A Modified direct power control strategy allowing the connection of three-phase inverter to the grid through LCL filters," *Proc. of 40th IAS Annual Meeting on Industrial Application Conference, China*, pp. 1-7, 2005.

[14] S. A. A. Fallahzadeh, N. R. Abjadi, A. Kargar, "Direct active and reactive power control of inverter-based DGs using adaptive input-output feedback linearization," *Proc. of Electric Power Distribution Conference*, pp. 1-7, 2016.

[15] S. Aurtenechea, M. A. Rodriguez, E. Oyarbide, J. R. Torrealday, "Predictive direct power control – a new control strategy for DC/AC converters," *Proc. of 32th Annual Conference on Industrial Electronics*, pp. 1661-1666, 2006.

[16] X. Liu, D. Wang, Z. Peng, "Predictive direct power control for three-phase grid-connected converters with online parameter identification," *International Transactions on Electrical Energy Systems*, vol. 27, pp.1-21, 2017.

[17] I. Colak, E. Kabalci, R. Bayindir, "Review of multilevel voltage source inverter topologies and control schemes," *Journal of Energy Conversion and Management, Elsevier*, vol. 52, pp. 1114-1128, 2011.

[18] A. T. Alsakhen, A. M. Qasim, B. Qaisieh, A. Elnady, "Experimental and simulation analysis for the 5-level diode clamped inverter," *Proc. of International Conference on Electric Power and Energy Conversion Systems*, 2015, pp. 1-4.